Direct growth of three-dimensional multicomponent micropatterns of vertically aligned single-walled carbon nanotubes interposed with their multi-walled counterparts on Al-activated iron substrates†

Liangti Qu and Liming Dai*

Received 28th February 2007, Accepted 16th May 2007
First published as an Advance Article on the web 24th May 2007
DOI: 10.1039/b703046k

Vertically aligned single-walled carbon nanotubes (VA-SWNTs) have been synthesized by an Al-activated plasma-enhanced chemical vapor deposition (PECVD) method. On this basis, we have developed a facile but effective method for direct growth of multicomponent micropatterns of VA-SWNTs interposed within the patterned areas surrounded by vertically aligned multi-walled carbon nanotubes (VA-MWNTs) onto an Al-activated iron substrate. The Al-activated iron substrate was prepared by region-selectively depositing an Al thin layer on either an Fe-coated substrate or a commercially available iron foil. This simple approach allows for an effective integration of various aligned carbon nanotubes with different electronic characteristics into multifunctional materials and devices.

Introduction

For many applications involving carbon nanotubes, it is highly desirable to prepare carbon nanotubes in an aligned and/or micropatterned form so that their structure/properties can be readily assessed while they can be effectively incorporated into multicomponent systems with potential synergetic effects.[1] Although the formation of aligned/micropatterned multi-walled carbon nanotubes (MWNTs) has been known for some years,[2] the synthesis of vertically aligned single-walled carbon nanotubes (VA-SWNTs) in either a patterned or a nonpatterned form is a recent development. The slow progress in the VA-SWNT growth is largely caused by the difficulty in preparing densely packed small catalyst particles ($\sim$1 nm in diameter) that do not aggregate into bigger ones at the high temperature required for the single-walled nanotube growth.[3–10] With the recent developments in nanoscience and nanotechnology, there is a pressing need to integrate multicomponent nanoscale entities into multifunctional materials and devices. In this context, we have previously reported a dry contact transfer technique[11] for preparing multicomponent carbon nanotube micropatterns, in which COOH-containing non-aligned MWNTs were region-selectively adsorbed within the heptylamine-plasma-treated areas interdispersed into the patterned structure of aligned MWNTs.[11,12] More recently, we have also demonstrated the formation of multicomponent carbon nanotube micropatterns with self-assembled non-aligned MWNTs interposed within the patterned structure of aligned SWNTs.[13] The integration of non-aligned MWNTs into either aligned MWNT or aligned SWNT micropatterns demonstrated above could lead to novel multicomponent/multifunctional materials and devices.

Department of Chemical and Materials Engineering, Department of Chemistry and UDRI, University of Dayton, Dayton, OH 45469, USA. E-mail: ldai@udayton.edu; Fax: +1 937 2293433; Tel: +1 937 2292670
† The HTML version of this article has been enhanced with colour images.

On the other hand, it is practically important to directly grow VA-SWNTs on metallic (conducting) substrates, especially for fabricating nanotube-based electronic devices. Much like the case with aligned MWNTs grown on metal substrates,[14] however, only a little effort has recently been made to grow vertically aligned SWNTs and double-walled carbon nanotubes on certain Ni-containing alloy foils *via* a water-assisted chemical vapour deposition (CVD) process using sequentially sputtered Al_2O_3 (30 nm)/Fe (1 nm) as catalyst.[15] Guided by some earlier studies on the preparation of stable Al-containing small catalyst particles,[3,7,16] we used here a thin layer of Al coating on commercially available iron foils (0.25 mm thick, Aldrich) or other Fe pre-coated substrates (*e.g.* SiO_2/Si wafer) to effectively minimize possible aggregation of the Fe catalyst particles formed *in situ* during the high-temperature and plasma-enhanced CVD (PECVD) growth of VA-SWNTs. We further found that micropatterns of VA-SWNTs interposed with their multi-walled counterparts were readily produced on either Fe-coated substrates or commercially available iron foils pre-coated with a patterned thin Al film, as reported below.

Experimental

Materials and characterization

Iron foils with a thickness of 0.25 mm were purchased from Aldrich, and Al thin coatings were prepared on a Denton Sputter coating system (Explorer 14). The coating thickness was determined by a Dektak 6M Surface Profiler. Scanning electron microscopic (SEM) and transmission electron microscopic (TEM) images were recorded on a Hitachi S-4800 high-resolution SEM and Hitachi H-7600 TEM unit, respectively. Raman spectra were obtained using an inVia micro-Raman spectrometer (Renishaw) with a 785 nm laser. Current–voltage measurements on the aligned carbon nanotubes grown on an Fe foil were performed using an EG&G potentiostat (model 263A).

Substrate preparation

For electropolishing, the iron foil acting as a cathode was first electrochemically activated by putting it into an aqueous mixture solution of Na_2CO_3 (25–30 g mL^{-1}), NaOH (20–25 g mL^{-1}), and Na_3PO_4 (25–30 g mL^{-1}), with a stainless steel sheet or nickel sheet being used as the anode. The applied voltage and current were controlled within 2–4 V and 0.3–0.5 A, respectively, for about 10–15 min. Thereafter, the iron foil was immersed into an aqueous solution of H_2SO_4 (27 wt%) and HC1 (10 wt%) for 5 min at 40–60 °C. After being thoroughly rinsed with deionized water, the iron foil was then placed into an electropolishing solution of H_3PO_4 (65 wt%), H_2SO_4 (15 wt%), CrO_3 (5 wt%), glycerol (12 wt%), and H_2O (3 wt%) as the cathode against a carbon bar anode. A voltage of 3 V and current of 0.5–0.6 A were applied for 10–25 min at 45–70 °C.

Al patterning by photolithography

For photolithographic patterning of Al, a thin layer of photoresist (3312 photoresist, 8 CPS, AZ) was spin-cast on an iron substrate (spinning speed: 4000 rpm). After annealing at 90 °C for 1 min, the substrate was exposed to UV light (350 nm, ~350 W) through a photomask. After removal of the photomask for selectively dissolving the photoresist within the UV-exposed areas in a developer solution (300 MIF Developer, AZ), the photoresist-patterned substrate was air dried and a thin layer of Al (1–5 nm) was then sputter-coated on the whole substrate surface. This was followed by acetone rinsing to completely dissolve the photoresist, leading to the formation of a micropatterned Al coating on the iron substrate for the subsequent nanotube growth, as shown in Fig. 2 (see later).

Carbon nanotube growth

VA-SWNTs were synthesized by pre-coating a thin layer of Al (1–5 nm) on Fe (or Fe-coated) substrates, followed by PECVD (80 W, 13.56 MHz) of 5 mTorr C_2H_2 and 400–600 mTorr H_2 for 10–15 min at 750 °C. VA-MWNTs were also prepared on an Fe coated (3–5 nm) substrate (*e.g.* SiO_2/Si wafer) without the Al pre-coating under the same growth conditions.

For comparison of the electrical properties of VA-SWNTs and VA-MWNTs, we also grew VA-MWNTs on an iron foil pre-coated sequentially with a thin layer of Al (10 nm) and a 3 nm Fe film by the PECVD process under similar conditions as described above.

Results and discussion

In a typical experiment, VA-SWNTs were synthesized on an Al-activated commercially available bulk iron foil (or an Fe-coated SiO_2/Si wafer) by PECVD (80 W, 13.56 MHz) of 5 mTorr C_2H_2 and 400–600 mTorr H_2 for 10–15 min at 750 °C. Fig. 1a shows the spot-like growth of non-aligned MWNTs or amorphous carbon fibers only on the pristine commercially available Fe foil. This is also confirmed by the corresponding Raman spectrum given in Fig. 1d. As seen in Fig. 1d, there is a strong D band centered around 1300 cm^{-1}, characteristic of amorphous carbon, with a relatively weak G band over 1500–1700 cm^{-1} arising from the multi-walled carbon nanotube structure. Upon coating with a thin layer (~2 nm) of Al, however, the same Fe foil supported the growth of carbon nanotubes (Fig. 1b). The non-uniform coverage of the poorly aligned nanotubes seen in Fig. 1b resulted, most probably, from an ineffective nanotube growth on the rough, and possibly contaminated, surface of the underlying commercial Fe foil. In contrast, well-aligned carbon nanotubes (~3 μm long) uniformly grew on the same commercially available Fe foil after electropolishing (see Experimental section) prior to the Al coating (Fig. 1c). The Raman spectrum of the nanotube sample shown in Fig. 1c recorded with a 785 nm laser (Fig. 1e) clearly shows the resonant radial breathing modes (RBMs) in the range of 130–280 cm^{-1} for SWNTs.[17] The clearly separated doublet at *ca.* 1570 and 1600 cm^{-1} seen for the G band in Fig. 1e is also a characteristic feature of SWNTs. A

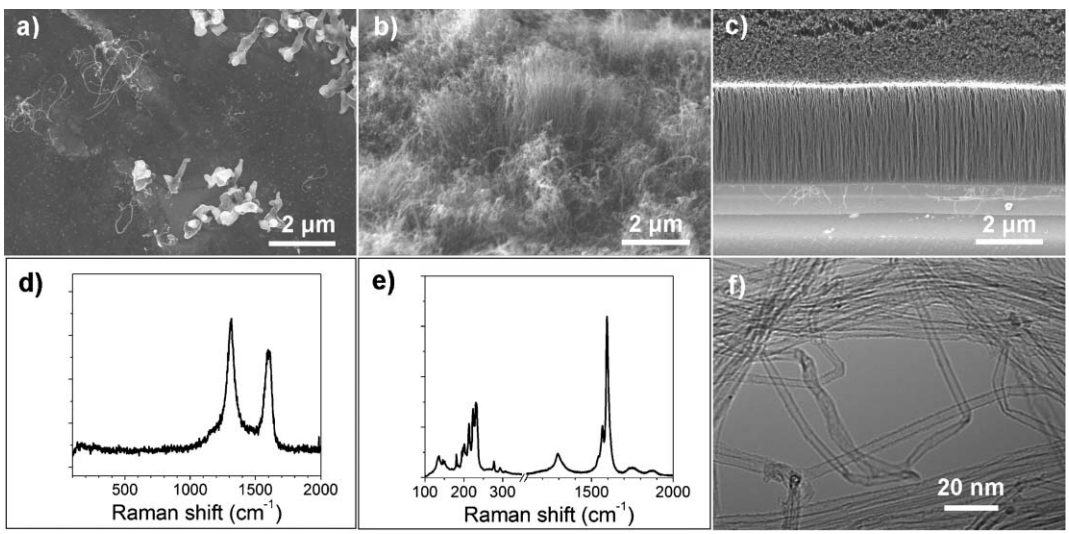

Fig. 1 a–c) Scanning electron microscopic (SEM) images of an Fe foil without (a) and with Al pre-coating (b, commercial iron foil; c, electropolished iron foil) after the nanotube growth. d) and e) Raman spectra of the as-grown nanotubes shown in a) and c), respectively. f) A TEM image of the as-grown nanotubes shown in c).

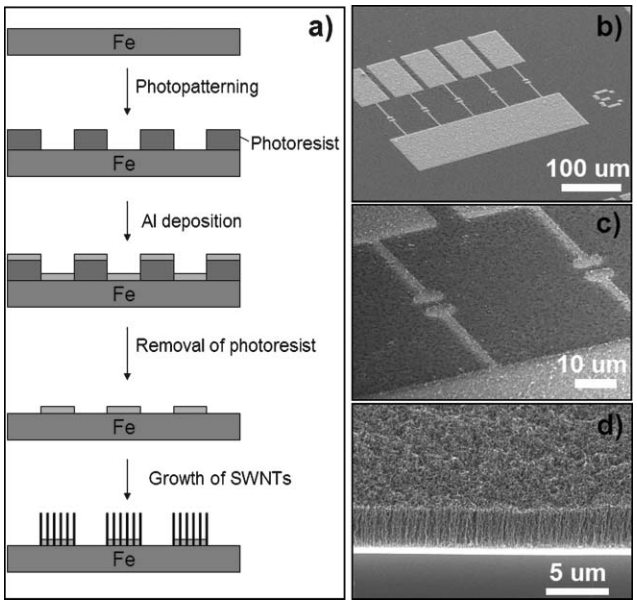

Fig. 2 a) Schematic representation of photopatterning Al on a commercially available iron foil for the growth of VA-SWNTs. b) and c) Top views of the VA-SWNT micropattern at different magnifications. d) A side view of the VA-SWNT micropattern at a higher magnification.

transmission electron microscopic image of individual nanotubes from an ethanol dispersion of the sample shown in Fig. 1c reveals, once again, the SWNT structure (Fig. 1f). With the Al-activation, therefore, we have successfully synthesized VA-SWNTs on the commercially available iron foil, which otherwise cannot support VA-SWNT growth.

On the above basis, we proceeded to grow VA-SWNT micropatterns by region-selectively coating a thin layer of Al on the bulk iron substrate. As shown in Fig. 2a, we used a photopatterning method, as described in detail in the Experimental section, to region-selectively deposit Al on the commercially available bulk iron foil, after electropolishing, for patterned growth of VA-SWNTs. Fig. 2b and c show the top-view SEM images recorded at different magnifications for the VA-SWNT micropattern thus prepared, while a cross-section view of the same aligned nanotube array is given in Fig. 2d. As can be seen, VA-SWNT micropatterns having a close replication of the photomask structure with well-aligned nanotubes growing only in the Al covered regions, suitable for microelectronic device fabrication, are clearly evident.

Apart from the growth of VA-SWNTs on iron foils by the Al activation described above, we also found that thin Fe catalyst coating (3–5 nm) on conventional substrates (*e.g.* SiO_2/Si wafer) used for the growth of VA-MWNTs (Fig. 3a and c) can also be activated to grow VA-SWNTs by pre-coating with a thin layer of Al (Fig. 3b and d). This finding, together with Al patterning, enabled us to readily prepare multicomponent micropatterns with the Al-activated VA-SWNTs interposed within the patterned VA-MWNT arrays on an Fe pre-coated substrate (*e.g.* SiO_2/Si wafer).

Fig. 4a shows the steps for patterned deposition of an Al thin coating through a TEM grid (as the physical mask) onto a SiO_2/Si wafer pre-coated with a 3 nm Fe film to support the

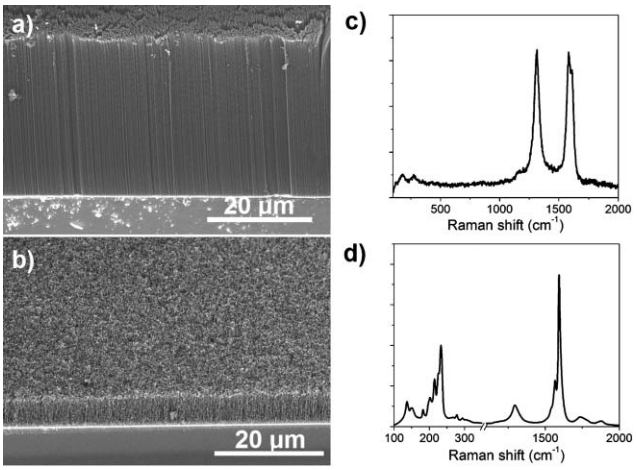

Fig. 3 SEM images and Raman spectra of aligned carbon nanotubes formed on 3 nm Fe-coated SiO_2/Si wafers without (a, c) and with (b, d) a 2 nm Al pre-coating.

region-selective growth of VA-SWNTs over the Al covered areas and VA-MWNTs in the Al-free regions. Fig. 4b shows a top view of the resultant nanotube micropattern, in which the hexagonal windows of the TEM grid "mask" were replicated. The corresponding side view in Fig. 4c clearly shows the shorter VA-SWNTs interposed within the hexagonal areas surrounded by longer VA-MWNTs. The single-walled and multi-walled nanotube characteristics of those shorter VA-SWNTs and longer VA-MWNTs within the three-dimensional (3-D) multicomponent nanotube micropatterns shown in Fig. 4b and c were confirmed by area-selected micro-Raman spectra (spot size $\approx$ 2 μm). To obtain more detailed information on the 3-D nanotube micropattern formation, we undertook a close examination of the growth process by taking SEM images at different growth periods. We found that the VA-SWNTs grew faster than the surrounding VA-MWNTs at the initial stage up to several microns within

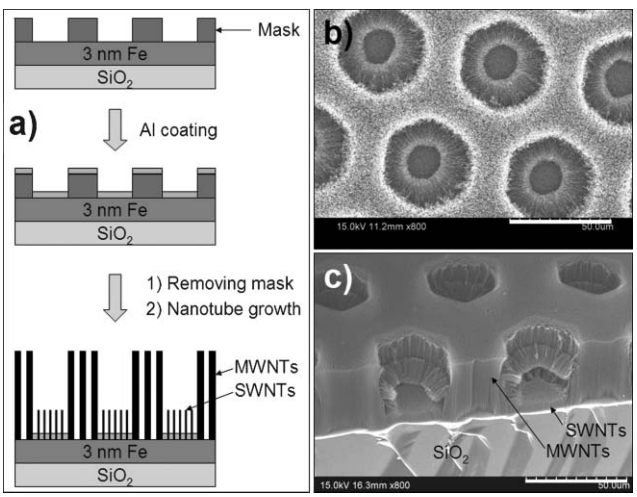

Fig. 4 a) Schematic representation of Al patterning on an Fe-coated substrate for the patterned growth of three-dimensional interposed VA-SWNTs and VA-MWNTs. b) and c) Top and cross-section views of the 3-D VA-MWNT/VA-SWNT micropatterns. Scale bars: 50 μm.

1–2 min (Fig. 5a and b). At the growth time of *ca.* 8 min, the VA-MWNTs became taller than VA-SWNTs (Fig. 5c and d). Further increase in the growth time caused a continuous growth of the VA-MWNTs while the height of the VA-SWNTs remained unchanged (Fig. 5e and f). Compared with VA-MWNTs, therefore, it seemed that the VA-SWNTs showed a faster growth speed and a shorter growth lifetime. This is because the smaller catalyst particles for the SWNT growth possess a higher surface to volume ratio, and hence an enhanced supply of carbon source for the initial fast nanotube growth. The larger surface area for the smaller catalyst particles also caused an increased susceptibility of surface contamination to poison the catalyst activity for a short growth lifetime. The interplay of the above two factors is responsible for the observed length differences between those VA-SWNTs and VA-MWNTs in the resultant 3-D multi-component nanotube micropatterns.

It is also interesting to note that those VA-MWNTs adjacent to the VA-SWNTs around the edge of the hexagonal windows bent toward the window center, resulting in the formation of a hollow cover over the VA-SWNTs within the hexagonal window (Fig. 4b and c and Fig. 5d–g) due probably to mismatches in the growth rate and strength of the van der Waals (vdW) forces between the VA-SWNTs and VA-MWNTs at their interface. The difference in the nanotube growth rates could cause the further growing MWNTs to be "pulled" down by the "dead" SWNTs at the edge of the hexagonal windows through possible interfacial entanglements between the single-walled and multi-walled nanotubes at the late growth stage (Fig. 5d, f, and g). Although the detailed formation mechanism for the bent aligned MWNTs is pending further study, the above description seems to be supported by the observation that some of the curved MWNTs were still connected with the VA-SWNTs after the bending, and that the overall length of the bent nanotubes is similar to that of the VA-MWNTs (Fig. 5g). In order to understand why VA-WMNTs can grow on substrates pre-coated with a thin layer of iron whereas the pristine bulk iron foil cannot support the aligned nanotube growth, we have further undertaken a high-resolution SEM examination of the surface of both the bulk iron foil and a SiO_2/Si wafer-supported Fe thin coating during the heating process required for the nanotube growth, but deliberately eliminated the carbon source. Our preliminary results indicate that densely packed Fe nanoparticles ($\sim$20 nm) of the size suitable for the growth of VA-MWNTs could form from the thin Fe-coating but not on the bulk iron foil under the current conditions. The above observed difference could be attributed to different particle nucleation processes on these two different iron substrates.

Unlike the 3-D single-component VA-MWNT micropatterns reported earlier,[18] the newly prepared 3-D multicomponent VA-MWNT/VA-SWNT micropatterns should show even more interesting region-specific electronic properties attractive for fabricating multifunctional micro-/nano-electronics with region-specific features while the conducting substrate provides a direct electrical contact. Indeed, our preliminary results from the *I*–*V* measurements on the non-patterned VA-SWNT and VA-MWNT arrays, using a sputter-coated gold layer on the top of the nanotube film as a counter electrode (inset of Fig. 6), indicate semiconducting and metallic behaviors for the VA-SWNTs and VA-MWNTs, respectively (Fig. 6).

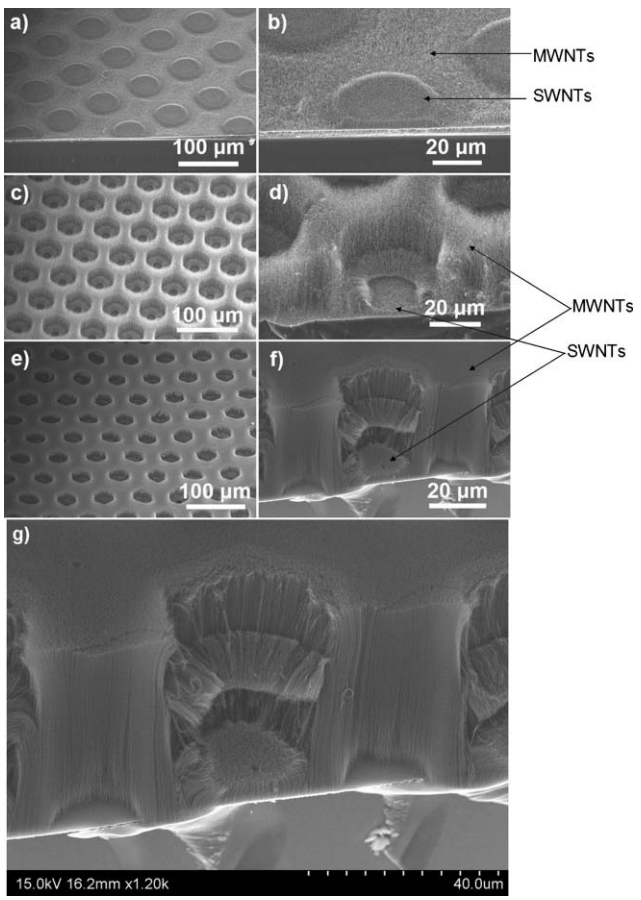

Fig. 5 Tilt and side SEM images of hybrid patterned growth of aligned SWNTs and MWNTs with different magnifications at different growth times. a, b) 1–2 min; c, d) 8 min; e, f) 15 min, and g) a higher magnification view of f).

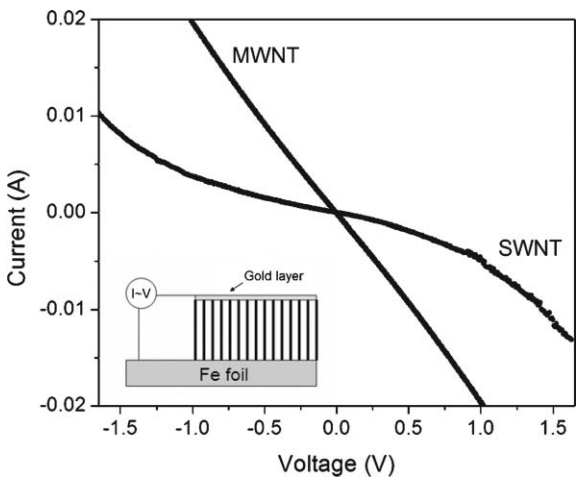

Fig. 6 Current (*I*)–voltage (*V*) curves of the as-grown non-patterned VA-SWNTs on a 2 nm Al coated Fe foil and VA-MWNTs on an Fe foil pre-coated sequentially with a thin layer of Al (10 nm) and a 3 nm Fe film.

Conclusions

We have demonstrated a facile but effective method for Al-activated syntheses of VA-SWNTs by coating a thin layer of Al on either commercially available iron foils or substrates pre-coated with an Fe nanofilm. We further found that substrates pre-coated with an Fe nanofilm conventionally used for the growth of VA-MWNTs can also be activated by a thin layer of Al to support the VA-SWNT growth. These findings, together with the region-selective deposition of an Al thin layer on either bulk iron foils or Fe-nanofilm-coated substrates, have enabled us to produce not only pure VA-SWNT micropatterns directly on the iron foil but also three-dimensional multi-component micropatterns with VA-SWNTs interposed within the patterned areas surrounded by VA-MWNTs. Therefore, this simple approach is of practical significance as it allows the direct growth of aligned carbon nanotubes on various conducting substrates and an effective integration of various aligned carbon nanotubes with different electronic characteristics into multidimensional/multifunctional materials and devices.

Acknowledgements

The authors acknowledge the support from NSF (CMS-0609077) and AFOSR (FA9550-06-1-0384).

References

1 *Carbon Nanotechnology: Recent Developments in Chemistry, Physics, Materials Science and Device Applications*, ed. L. Dai, Elsevier, Amsterdam, 2006.
2 See, for example: (*a*) B. Q. Wei, Z. J. Zhang, G. Ramanath and P. M. Ajayan, *Appl. Phys. Lett.*, 2000, **77**, 2985; (*b*) Z. J. Zhang, B. Q. Wei, G. Ramanath and P. M. Ajayan, *Appl. Phys. Lett.*, 2000, **77**, 3764; (*c*) Y. J. Jung, B. Q. Wei, R. Vaitai and P. M. Ajayan, *Nano Lett.*, 2003, **3**, 561; (*d*) B. Q. Wei, R. Vajtai, Y. Jung, J. Ward, R. Zhang, G. Ramanath and P. M. Ajayan, *Nature*, 2002, **416**, 495; (*e*) W. Z. Li, S. S. Xie, L. X. Qian, B. H. Chang, B. S. Zou, W. Y. Zhou, R. A. Zhao and G. Wang, *Science*, 1996, **274**, 1701; (*f*) Z. W. Pan, S. S. Xie, B. H. Chang, C. Y. Wang, L. Lu, W. Liu, W. Y. Zhou and W. Z. Li, *Nature*, 1998, **394**, 631; (*g*) S. Fan, M. G. Chapline, N. R. Franklin, T. W. Tomber, A. M. Cassell and H. Dai, *Science*, 1999, **283**, 512; (*h*) C. N. R. Rao, R. Sen, B. C. Satishkumar and A. Govindaraj, *Chem. Commun.*, 1998, 1525; (*i*) Z. F. Ren, Z. P. Huang, J. H. Xu, P. B. Wang, M. P. Siegal and P. N. Provencio, *Science*, 1998, **282**, 1105; (*j*) L. Dai, A. Patil, X. Y. Gong, Z. X. Guo, L. Q. Liu, Y. Liu and D. B. Zhu, *ChemPhysChem*, 2003, **4**, 1150 and references cited therein; (*k*) L. T. Qu, Y. Zhao and L. Dai, *Small*, 2006, **2**, 1052; (*l*) C. Wei, L. M. Dai, A. Roy and T. B. Tolle, *J. Am. Chem. Soc.*, 2006, **128**, 1412; (*m*) Y. Yan, M. B. Chan-Park and Q. Zhang, *Small*, 2007, **3**, 24.
3 K. Hata, D. N. Futaba, K. Mizuno, T. Namai, M. Yumura and S. Iijima, *Science*, 2004, **306**, 1362.
4 G. Zhang, D. Mann, L. Zhang, A. Javey, Y. Li, E. Yenilmez, Q. Wang, J. P. McVittie, Y. Nishi, J. Gibbons and H. Dai, *Proc. Natl. Acad. Sci. U. S. A.*, 2005, **102**, 16141.
5 E. Gyula, A. A. Kinkhabwala, H. Cui, D. B. Geohegan, A. A. Puretzky and D. H. Lowndes, *J. Phys. Chem. B*, 2005, **109**, 16684.
6 T. Iwasaki, G. F. Zhong, T. Aikawa, T. Yoshida and H. Kawarada, *J. Phys. Chem. B*, 2005, **109**, 19556.
7 Y. Q. Xu, E. Flor, M. J. Kim, B. Hamadani, H. Schmidt, R. E. Smalley and R. H. Hauge, *J. Am. Chem. Soc.*, 2006, **128**, 6560.
8 M. Cantoro, S. Hofmann, S. Pisana, V. Scardaci, A. Parvez, C. Ducati, A. C. Ferrari, A. M. Blackburn, K. Y. Wang and J. Robertson, *Nano Lett.*, 2006, **6**, 1107.
9 Y. Murakami, S. Chiashi, Y. Miyauchi, M. H. Hu, M. Ogura, T. Okubo and S. Maruyama, *Chem. Phys. Lett.*, 2004, **385**, 298.
10 L. Zhang, Y. Q. Tan and D. E. Resasco, *Chem. Phys. Lett.*, 2006, **422**, 198.
11 J. Yang, L. Dai and R. A. Vaia, *J. Phys. Chem. B*, 2003, **107**, 12387.
12 L. Dai and A. W. H. Mau, *Adv. Mater.*, 2001, **13**, 899.
13 J. Yang, L. Qu, Y. Zhao, Q. Zhang, L. Dai, J. W. Baur, B. Maruyama, R. A. Vaia, E. Shin, P. T. Murray, H. Luo and Z. Guo, *J. Nanosci. Nanotechnol.*, 2007, **7**, 1573.
14 (*a*) B. A. Wang, X. Y. Liu, H. M. Liu, D. X. Wu, H. P. Wang, J. M. Jiang, X. B. Wang, P. A. Hu, Y. Q. Liu and D. B. Zhu, *J. Mater. Chem.*, 2003, **13**, 1124; (*b*) S. Talapatra, S. Kar, S. K. Pal, R. Vajtai, L. Ci, P. Victor, M. M. Shaijumon, S. Kaur, O. Nalamasu and P. M. Ajayan, *Nat. Nanotechnol.*, 2006, **1**, 112.
15 T. Hiraoka, T. Yamada, K. Hata, D. N. Futaba, H. Kurachi, S. Uemura, M. Yumura and S. Iijima, *J. Am. Chem. Soc.*, 2006, **128**, 13338.
16 (*a*) W. Wongwiriyapan, M. Katayama, T. Ikuno, N. Yamauchi, T. Mizuta, T. Murakami, S. Honda, K. Oura, K. Kisoda and H. Harima, *Jpn. J. Appl. Phys.*, 2005, **44**(1A), 457; (*b*) T. Komukai, K. Aoki, H. Furuta, M. Furuta, K. Oura and T. Hirao, *Jpn. J. Appl. Phys.*, 2006, **45**(7), 6043; (*c*) T. Komukai, K. Aoki, H. Furuta, M. Furuta, K. Oura and T. Hirao, *Jpn. J. Appl. Phys.*, 2006, **45**(11), 8988.
17 H. Telg, J. Maultzsch, S. Reich, F. Hennrich and C. Thomsen, *Phys. Rev. Lett.*, 2004, **93**, 177401.
18 A. Patil, T. Ohashi, A. Buldum and L. Dai, *Appl. Phys. Lett.*, 2006, **89**, 103103.